energies

MDPI

Article

University Campus and Surrounding Residential Complexes as Energy-Hub: A MILP Optimization Approach for a Smart Exchange of Solar Energy

Sergio Rech [1,*], Stefano Casarin [2], Carlos Santos Silva [3] and Andrea Lazzaretto [2]

[1] Veil Energy, 35010 Padova, Italy
[2] Department of Industrial Engineering—University of Padova, 35131 Padova, Italy; stefano.casarin.3@phd.unipd.it (S.C.); andrea.lazzaretto@unipd.it (A.L.)
[3] Department of Mechanical Engineering—Technical University of Lisbon, 1049-001 Lisbon, Portugal; carlos.santos.silva@tecnico.ulisboa.pt
* Correspondence: s.rech@veil-energy.eu

Received: 27 April 2020; Accepted: 3 June 2020; Published: 6 June 2020

Abstract: An effective way to enlarge the utilization of renewable energy consists in creating a correct interface between producers, consumers, and storage devices, i.e., a so-called "energy hub". This opens a difficult challenge, especially in the urban areas where the availability of room for the installation of renewable plants is limited. This paper considers a university campus in the center of Lisbon that requires a significant amount of electricity and natural gas to support the internal activities. The idea is to fulfil part of the energy consumption of the campus with the excess of energy supplied by solar systems installed in the surrounding residential buildings. The goal is to find the number and type of solar equipment that maximize the reduction of annual energy costs of both residents and campus, where the campus is seen as a virtual storage. Results of the optimization show that, considering the best-exposed 100 buildings in a radius of 500 m around the campus, the campus can reduce the annual energy expenses up to 8.61%, whereas the money-saving for the residents is of the order of 24% to 29%, depending on solar exposure. A sensitivity analysis shows also the higher benefits for both the campus and users deriving from expected decreasing costs of photo-voltaic (PV) panels.

Keywords: solar energy; photo-voltaic; solar-thermal collectors; mixed integer linear programming; configuration optimization

1. Introduction

The Instituto Superior Técnico (IST) is one of the most prominent academic institutions in Portugal and boasts several partnerships with renowned universities all over the world, together with a prolific academic research activity. It has three campuses, the main one being the Alameda campus, situated in the center of Lisbon.

The Alameda Campus was situated in the outskirts of Lisbon, but with the city's expansion in the first half of the twentieth century, it quickly became surrounded by multiapartment buildings. The IST works all year long, except for two weeks of August, and requires a high amount of energy for didactic, administrative, and research activities. An internal energy audit revealed that the energy mix is composed for 81% of electrical energy (EE), while 19% is natural gas (NG). The energy consumption represents a relevant share of the yearly budget, and to this date, it only relies on the connection to the electric grid and NG distribution network. The campus does not perform any self-generation.

A way to reduce the energy-related costs and decrease the respective carbon footprint would be the integration of renewable energy source (RES) generators.

Portugal is a country with an abundant availability of RES: in 2016, the gross wind electric generation was 12,474 GWh [1], while the yearly sum of global irradiation collected with an optimally sloped surface was estimated greater than 2000 kWh/m^2 [2].

Solar energy is the selected RES, because the campus is surrounded by residential buildings, the roofs of which are not yet equipped either with solar photo-voltaic (PV) or with thermal (ST) collectors; the produced energy can be conveyed in low voltage thanks to the short distances.

1.1. State of the Art

The concept of an energy hub (EH) can be defined as [3] "an interface between consumers, producers, and storage devices: directly or via conversion equipment, handling one or several carriers". Under this perspective, IST Campus has the potential to become an EH thanks to a careful design of the generators and their schedules.

Several approaches and optimization techniques have been applied successfully in the literature to the design and operation scheduling of EHs, polygeneration systems, distributed generation, and microgrids [3–6]. The energy hub concept was used in [7] to utilize renewable energy sources in the district heating systems, building and district conversions, and storage technologies at the neighborhood level to lower peaks in the energy demands of neighborhoods on the electrical grid and to reduce the overall consumption. Sigarchian et al. developed a model to find the optimal operating schedule of a polygeneration system using particle swarm optimization [8]. Fetanat and Khorasaninejad have used an ant colony optimization algorithm to design a hybrid PV-wind energy system, comparing it with other optimization methods [9]. Christidis et al. found the optimal size of heat storage devices, as well as the operation of several power plant units, by a mixed-integer programming (MIP) approach [10]. Similarly, Rech and Lazzaretto used a mixed-integer linear programming (MILP) approach to find the optimal operating schedule of RES converters and the size of the energy storage devices of a small municipality [11]. Rech [12] generalized this approach to provide guidelines and practical examples for formulating the dynamic optimization problem of the design and operation of a fleet of energy conversion and storage units.

In this paper, a MILP model has been developed to design a decentralized energy production network relying on solar energy. A MILP model has been chosen, because it has the advantage that—when convergence is attained—it is proven for the feasible solution to be optimal or close to optimal [13]. MILP is also being extensively used for energy hub models for being fast and reliable [14].

In the literature, there are several software and languages commonly used to formulate and solve MILP problems. Distributed energy resources–customer adoption model (DER-CAM) is a powerful tool developed by Berkeley Lab. It formulates problems as a MILP and finds globally optimal solutions for distributed energy resource investments for either buildings or multi-energy microgrids [15]. This tool has been thoroughly used to find the optimal design and configurations of DER systems [16–18].

There are other tools to model and solve complex optimization problems: general algebraic modeling system (GAMS) is a modeling system for mathematical programming and optimization and is suitable for modeling several types of problems and supports a large variety of solvers [19]. Other suitable languages to develop DER models (among others) are: C, C++, Java, Python, and MATLAB. The most used solvers for MIP, MILP, and other nonlinear problems are CPLEX and GUROBI [20,21].

1.2. Objectives

The aim of this work is to assess the economic feasibility of the implementation of a decentralized renewable energy system that ensures a reduction in the energy-related costs. For a set of residential complexes around the campus (IST), this translates in:

- finding the optimal configuration of the energy generation system, i.e., the amount of installed PV modules, ST collectors, and size of the thermal storage (TS) tank (if any) in the residential

complexes that produces a reduction of the energy-related expenses for both the campus and the residents, and
- finding the optimal operation strategy of this energy generation system.

The investment and operation and management (O&M) costs are accounted as part of the IST yearly energy expenses, because the project is supposed to be fully financed by IST.

Four multifamily residential complexes, each representing a category of buildings, are selected for the energy exchange with the campus. The results obtained for a single building are then scaled for the estimated number of edifices having similar characteristics (i.e., belonging to that category of buildings), so assessing the global-saving potential.

If the conditions are favorable, IST and the owners of the apartments to which the rooftops belong will form a synergistic cooperative: the former will get electricity or thermal energy that is not self-consumed, while the latter receive free renewable energy by making available the unused roof surface.

The reason for considering the ST technology is that, in Portugal, it is common to use EE for heating purposes: a ST system would reduce the renewable PV energy self-consumption, allowing more EE to feed IST.

As stated above, the following aspects will be considered:

- The amount and type of the energy conversion devices to be installed: IST can achieve a cheaper price per device than single families, given the higher amount of electricity it takes from the grid compared to a regular household, and
- the buildings to be selected for the partnership. Each building is characterized by several parameters defining the surface availability and its quality (a north-facing rooftop is less valuable than a nonshaded south-facing roof), as well as a number of apartments that have an energy consumption profile, the economic conditions to which IST receives the EE from the buildings (name in the following "users", USRs) and vice-versa.

2. Methods

In this section, the main procedures for the characterization of the system are presented. In Section 2.1, the system is described: the main hypotheses are shown, as well as the procedures to model IST and the USR energy consumption profiles. In Section 2.2, the generation of solar energy is described. Eventually, in Section 2.3, the construction of the model is presented in detail.

2.1. System Description

The system is modeled as a central consumption node (the campus, IST) surrounded by residential complexes (USRs) that can become generation nodes and that, if so, will connect to it radially. Figure 1 shows the possible interactions between IST, a generic USR, and the electric grid. As shown, there can be an energy flow between IST and a USR. The arrows represent the possible directions of the energy flows (defined as P). Superscripts and subscripts are to be read as "from-to", respectively.

The IST campus has a peak of EE consumption of 1 to 2 orders of magnitude greater than that of a single-family household. IST can be considered as a fictitious electricity storage system: with the exceeding EE produced by the oversized PV modules, the USRs "charge" the campus, which—when there is not solar energy production—can return the charged energy back to the respective USR. This is because IST generally pays a lower price per kWh than a common household.

The analysis is performed on a yearly basis, with 1h resolution. With 8760 times the steps to simulate a year, the computational effort (the solving time) would be too high. This is why it has been chosen to reduce the year to 4 representative "design" days, one for each season. This choice reduces greatly the complexity of the model.

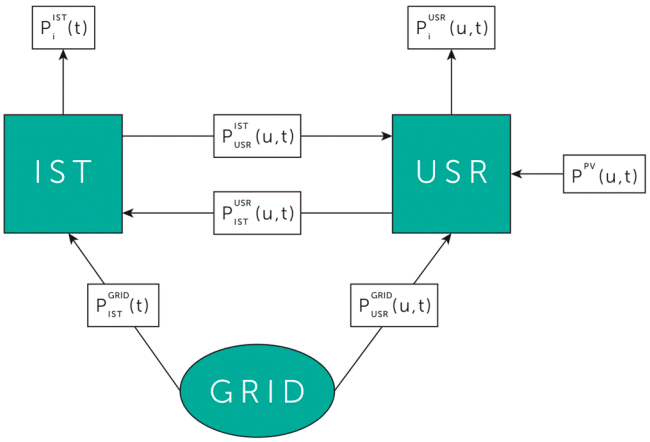

Figure 1. Representation of the system: possible interactions between Instituto Superior Técnico (IST), a generic building (USR), and the electric grid.

2.1.1. IST Energy Characterization

IST Campus is situated on the top of a hill and is composed of a total of 26 buildings [22], in which didactic, research, or administrative activities take place.

IST is characterized by an hourly electric energy demand. The "Campus Sustentável" project of IST [23] provided a file of hourly records of the campus electric demand. The measurements cover a time range from December 2015 to November 2017.

The raw data has been treated by removing the not-a-number (NaN) records. All the values that fall outside a 3σ (99.7% confidence) interval are removed, because they are considered outliers, which are unusual values whose existence is led back to random malfunctions of the measurement instruments and are not related to the phenomena of interest.

The records are grouped into seasons: winter ranges from 21/12 to 20/03, spring from 21/03 to 20/06, and so on for summer (the records of the month of August have been excluded; the two-week closure and the absence of didactic activities make the month not representative of IST normal functioning) and autumn. This division of the year into seasons is consistent with the environmental records, as explained later on in this section.

For each season, the records are grouped again by the hour of the day in which they were taken. For each of the 24 sets of each season, the median value is extracted; this value will be the value of the respective hour of the design day. The median has been preferred to the mean value due to its higher robustness and lower sensitivity on the extremes.

The obtained curves (Figure 2) show that the daily EE consumption of the campus is rather constant along the year. This is consistent with the behavior of the campus, since it works during 11 months per year (in August, the main activities are suspended). The base load is 800 kW, while the peak load is approximately 2.2 kW.

2.1.2. USRs Characterization

The city of Lisbon is made of thousands of buildings; their individual assessment (single and multifamily residential, nonresidential, etc.) would require an in-depth analysis that is outside the scope of this work. It has been chosen to limit the number of buildings (USRs) to four.

The four USRs have been chosen following these criteria:

1. vicinity to IST: lower distances mean lower losses; therefore, the search for rooftops shall be focused on the surroundings of the campus,
2. incident solar radiation: surfaces that receive large amounts of solar radiation over the year are more attractive than the others, and

3. representativity: the four buildings should not be unique, as the results from assessing a place belonging to a family of constructions can be expected to be similar for the whole family; this allows for the extension of the results for a single complex to several buildings.

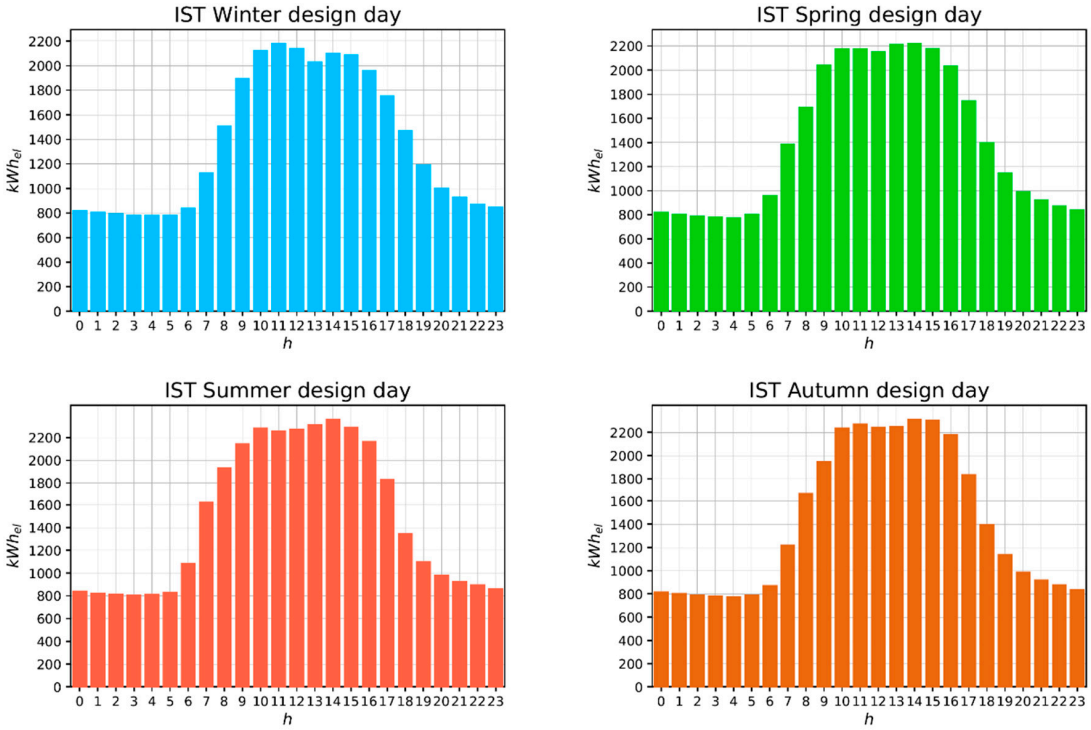

Figure 2. Electricity consumption of IST during the design day of each season.

They were all built between 1919 and 1945 and are referred as "Gaioleiro" buildings [24]; thus, similar energetic performances can be expected. From observation, the number of floors and apartments has been derived.

Information regarding the amount of incident solar radiation on their respective roofs, as well as their surface extensions, were retrieved from the solar energy potential map in Figure 3 [25]. This resource provides data regarding the characteristics of the roofs of the city of Lisbon.

Figure 3. Solar energy potential map of the area surrounding IST Campus [25].

Electric Load

Likewise, for IST, the hourly electric energy demand for each USR was obtained from different sets of measurements. This data was provided by the Center for Innovation, Technology and Policy Research (IN+) of IST, who performed a range of measurements promoted by ERSE (*Entidade Reguladora dos Serviços Energéticos*—Portuguese Energy Services Regulatory Authority) [26]. The project monitored the energy consumption of the nationwide participants to improve the efficiency in the residential sector. These data include the electricity consumption for lighting, household appliances, and space cooling, while the consumption for space heating (when provided by electric heaters) is considered separately.

Among all the records, those considered appropriate for the analysis are presented in Table 1. The same process shown in Section 2.1.2 to obtain seasonal design days has been adopted.

Table 1. Electric and thermal consumption profile association for each building (USR): *Ppl/flat* is the number of people living in the respective flat, N_{flats} is the amount of individual flats in each building, S_{roof} is the roof total surface, A_{wall} the external wall area, L heating loss coefficient, and TL_{sh} the daily thermal load requirement for space heating.

USR	*Ppl/flat*	N_{flats}	Type	S_{roof}	Roof Main Orientation	A_{wall}	L	TL_{sh}
				(m^2)		**(m^2)**	**(kW/m^2)**	**(kWh)**
1	4	4	T3	137.75	South	91.8	1.589	79.077
2	3	3	T3	100.25	East	64.8	1.051	69.727
3	3	3	T2	91.25	West	59.4	1.049	69.581
4	4	8	T4+	264	South	202.5	3.383	67.35

Due to the selective monitoring of the electric consumption of some appliances, the electric consumption is integrated with the energy consumption for space heating and domestic hot water (DHW). Even though the use of natural gas for DHW far exceeds the use of EE [26], it is assumed that each household only uses EE, for this means a higher electricity demand from the USRs; hence, less favorable conditions.

An electric profile has been eventually associated with each USR. The association is based on the following assumptions:

1. The electric profile is proportional to the number of inhabitants, so a reference profile (for one resident) has been obtained by dividing the available measured profile by the actual number of residents. The profile for USRs, including any number of residents, is then obtained by multiplying the reference profile by the selected number of residents, and
2. geometry (type in Table 1); occupancy (number of inhabitants); and routines are the same; the whole residential complex electrical consumption profile is equal to its number of flats times the hourly electric consumption of the respective electric profiles. The flat-type classification in Portugal is TN, where N means the number of rooms. Therefore, a T4 is a flat with four bedrooms, a kitchen, a living room, and a variable number of bathrooms. Similarly, a T2 has only two bedrooms, a bathroom, a kitchen, and so on.

Thermal Load

The daily thermal profile has been estimated with the base on the weather data provided by IST Meteorological Service, the Portuguese regulations [27], and assumed values of the buildings' global heat transfer coefficients. Each building under examination belongs to the district of São Jorge de Arroios in Lisbon. The values of the global heat transfer coefficients (U) of each building were taken from [24], in which, for each district of Lisbon, a statistical analysis was performed. In this work, the minimum, mean, maximum, and standard deviation values of the U for each district of Lisbon are provided. Since the difference between the mean and the maximum U-values is minimal, the

latter have been chosen for the analysis to be more conservative. The heating loss coefficient is then calculated following the procedure presented by Durmayaz et al. [28].

The thermal load is considered to be the result of two heating necessities: space heating (Q^{sh}) and domestic hot water (Q^{dhw}).

- The approach used to determine the energy necessity for space heating (SH) is the same as that by presented by Durmayaz et al.; the daily mean temperatures were calculated for every day of the year [28]. Their values have been plotted and fitted with a 6th-degree polynomial function and can be seen in Figure 4. The heating season starts and ends when the fitted function crosses the 15 °C value, respectively. The results are that the heating season ends on the 110th and begins on the 313th day, which corresponds to the 20th of April and 9th of November, respectively.

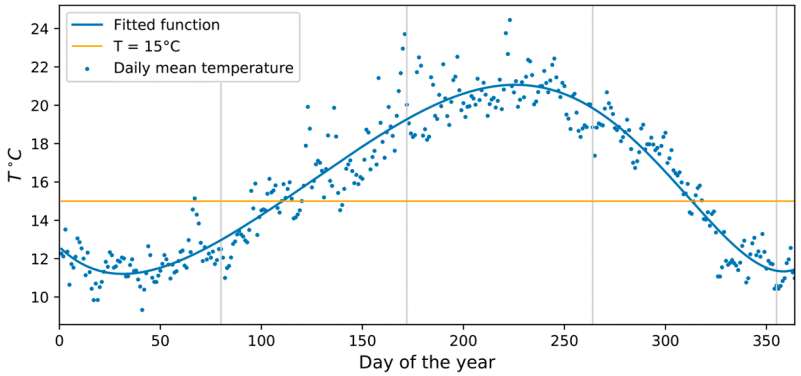

Figure 4. Yearly trend of the daily average temperatures. The vertical lines mark the ending of a season and the beginning of the next. Winter and summer cover the highest and lowest ranges of temperature levels, respectively, while spring and autumn cover the two transition periods.

The average temperature of every design day is above 15 °C, except for the winter one. The winter season is the only one entirely inside the heating season; therefore, the space-heating load will only be present for the winter design day. It is worth making a further correction: it is unusual for a Portuguese household to heat the entire flat. Q^{sh} is reduced by one-third to account for the nonheated parts of the respective flats.

Eventually, the normalized space-heating profile has been applied to obtain the daily space heating energy consumption.

- For the energy consumption for domestic hot water (DHW), the daily amount of energy has been calculated according to the Portuguese Regulations [29]. The municipal water feed temperature and the normalized profile for the DHW consumption were retrieved from [30].

If the total thermal load was fulfilled with EE (an electrical resistance of 98% efficiency), the overall electrical consumption profile for each USR in each design day would be the one presented in Figure 5. Note that the morning peak of electricity demand of each USR in the summer (Figure 4) is quite similar to that in the winter because of the high cooling demand in the hot season.

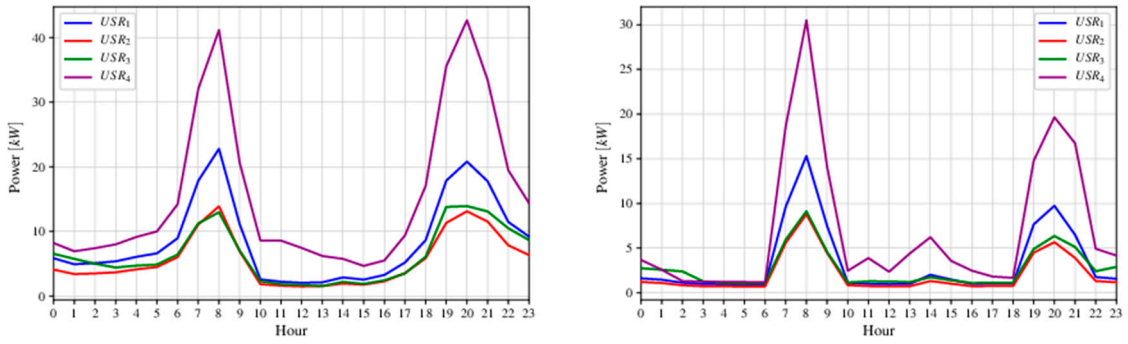

Figure 5. Overall electric load of each USR in the winter (**a**) and for the summer (**b**) season, assuming that the whole heat demand is fulfilled with electric energy.

2.2. Renewable Energy Generation

The specific solar energy production per unit equipment is modeled as a function of the solar radiation and ambient temperature. Both datasets have been recorded over a period of five years by the Meteorological Service of IST. The hourly records have been aggregated into one representative year through the median, with a process akin to that presented in Section 2.1.2.

The calculations implemented to obtain the total incident solar radiation on a tilted surface are the same as presented by Duffie and Beckman [31]. It is assumed that the modules will be oriented according to the normal of the façade of the building they will be installed on; therefore, each USR will have a different specific solar energy production profile.

2.2.1. PV Energy Generation

The selected PV technology is a monocrystalline silicon (mono-Si) panel manufactured by [32]. The power output of a PV module is modeled as a function of the incident solar radiation and the ambient temperature as proposed by Durisch et al. [33].

To each total solar radiation value, a specific (per module) electricity production for each USR is associated. The total output power of the installation is the algebraic sum of the output powers of the single modules. The inverter efficiency is assumed equal to 98%.

2.2.2. ST Energy Generation

The solar thermal energy output does not only depend on the physical properties of the collector itself but, also, on the inlet fluid temperature. This temperature changes according to the temperature inside the TS, which depends on the tank capacity and the energy subtraction from the users.

To keep the model simple and independent from the storage tank capacity (which is a decision variable of the optimization problem), the collector inlet temperature has been fixed at 60 °C. This is the minimum temperature allowed for the storage of hot water to avoid the proliferation of pathogens.

Typical solar flat plate collector performance parameters (optic and thermo-physical properties) were retrieved from [14].

Akin to Section 2.2.1, an hourly specific (per collector) thermal energy production is associated to each hour of the year.

2.3. Formulation of the Optimization Problem

The design optimization problem of the solar system is defined by taking into account its operation using a mixed-integer linear approach. The problem is written in a general form as:

$$\begin{aligned} &\text{find } \mathbf{x}^*(t) \text{ and } \boldsymbol{\beta}^*, \text{ which minimize } Z = f(\mathbf{x}(t)) \\ &\text{subject to } \mathbf{g}(\mathbf{x}(t), \boldsymbol{\beta}) = 0 \\ &\qquad\qquad \mathbf{h}(\mathbf{x}(t), \boldsymbol{\beta}) \leq 0, \end{aligned} \tag{1}$$

where:

- $\mathbf{x}(t)$ and $\boldsymbol{\beta}$ are the arrays of the continuous and integer/binary decision variables (the superscript * indicates their optimum value), respectively,
- Z is the objective function, and
- $\mathbf{g}(\mathbf{x}(t), \boldsymbol{\beta})$ and $\mathbf{h}(\mathbf{x}(t), \boldsymbol{\beta})$ are the equality and inequality constraints deriving from the model of the system.

The optimization problem was implemented in Python and solved using the MIP solver of GUROBI.

2.3.1. Decision Variables

All the integer/binary decision variables ($\boldsymbol{\beta}$ in Equation (1)) are associated with the design of the solar system configuration. Accordingly, their values are independent of time t (i.e., it is constant in the total optimization period). The variables belonging to this category of decision variables are:

- integer number of PV modules ($\sigma(u)$) and ST collectors ($\chi(u)$) to be installed on the roof of the user u [34], and
- binary variables used to impose the existence ($\alpha(u) = 0$) or not ($\alpha(u) = 1$) of the user u and, if so, whether the ST technology are to be implemented ($\varepsilon(u) = 1$) or not ($\varepsilon(u) = 0$) [35].

Among the design decision variables, there is also the continuous variable $V^{TS}(u)$ associated with the volume of the thermal storage (TS) equipment of each user u. [10–12,23]. The remaining continuous decision variables (**x**(t) in Equation (1)) are instead tied to the optimum operation of the system (their values can vary in the total optimization period). The set of the continuous decision variables includes:

- electrical ($P_B^A(u,t)$) and thermal ($Q_B^A(u,t)$) energy flows between the nodes ("A" is the starting node, and "B" is the arrival node),
- thermal energy flows charged to ($Q_{ch}^{TS}(u,t)$) or discharged from ($Q_{disch}^{TS}(u,t)$) the thermal storage or dissipated ($Q^{diss}(u,t)$) for each user u, and
- level of charge of the IST (see Equations (18) to (21)) and of the TS ($LVL(u,t)$), where u is the generic user in the set of the candidate users.

The problem has been defined so that the optimum value of the decision variables can only be either positive or null.

2.3.2. Fixed Parameters

In the optimization procedure, the fixed parameters (quantities that are known beforehand) are:

i. the hourly values of energy consumption and specific production for each node,
ii. the physical properties of the involved fluids (for the ST technology),
iii. the technological properties for each equipment (efficiencies), and
iv. the unitary prices/costs for the technologies and the electrical energy.

About point (iv) above, the specific cost per watt-peak of a PV module includes the cost for the module itself, the auxiliaries, and the installation costs. Its value has been chosen as the most expensive

cost found in [36]. The price of the electricity varies with the hour of the day. IST has a 4-phase tariff contract with the energy provider:

1. *ponta* (peak tariff, from 09:00 to 10:30 and from 18:00 to 20:30);
2. *cheia* (shoulder tariff, from 08:00 to 09:00, from 10:30 to 18:00, and from 20:30 to 22:00);
3. *vazio* (off-peak tariff, 00:00 to 02:00, from 06:00 to 08:00, and from 22:00 to 00:00); and
4. *super vazio* (minimum tariff, from 02:00 to 06:00).

For IST *ponta* phase, the price is composed of two parts: the energy component (0.112 €/kWh) and the power component (0.215 €/kW). Since the model is based on an hourly time-step, it is possible to sum the two components and obtain an overall price per kWh.

All the USRs have a 2-phase tariff: *vazio* (off-peak tariff) and *fora de vazio* (peak tariff), the former lasting from 22:00 to 08:00.

In the following, all fixed parameters are identified by the accent "ˆ" above the parameter symbol.

2.3.3. Objective Function

The objective function to be minimized (Z in Equation (1)) is the IST annual costs for energy, as the sum of (Equation (2)):

1. The actualized investment and O&M costs (the latter is expressed as a percentage of the former) for the equipment installed onto all USRs, $C_{inv+O\&M}$.
2. The overall cost for purchasing electricity from the grid, $C_{el,GRID}$.
3. The negative absolute value associated with the revenues from the sale of electricity to the USRs, Rev^{IST}_{USR}.

$$Z = \sum_{s}\left(\sum_{u}\left(C_{inv+O\&M}\cdot\frac{1}{365}+C_{el,GRID}-Rev^{IST}_{USR}\right)\cdot N_{days}\right),\ \forall s \in \{\text{seasons}\}. \tag{2}$$

The investment cost for the PV appliances is proportional to the peak wattage of the selected PV technology (Wp), which, in this case, is equal to 290 Wp [32], whereas, for the ST equipment, it is the sum of the costs of the collector and thermal storage.

2.3.4. Model of the System

Constraints are linear function setting conditions that variables are required to satisfy. In this problem, the constraints ($\mathbf{g}(\mathbf{x}(t),\boldsymbol{\beta})$ and $\mathbf{h}(\mathbf{x}(t),\boldsymbol{\beta})$ in Equation (1)) are used to impose the conditions under which the system can exist and operate, such as the energy balances and flows management, usage of the available roof surface, and economic conditions.

Energy Balances

Three types of energy balances are written: the electric energy balance of the IST (Equation (3)), a "local" electric energy balance for each USR (Equation (4)), and the only thermal energy balance of IST (Equation (7)). Local thermal energy balance of the USRs are not required, because the possibility to develop a district heating network is not contemplated in this work.

IST electric energy balance:

$$\hat{P}^{IST}_{L}(t)+\sum_{u}P^{IST}_{USR}(u,t)-\hat{\eta}_{el,t}\cdot\sum_{u}P^{USR}_{IST}(u,t)-P^{GRID}_{IST}(t)=0. \tag{3}$$

where $\hat{\eta}_{el,t}$ is the average efficiency of the two-way electric transition USR–IST (0.98).

USR electric energy balance:

$$P^{USR}_{L}(u,t)+P^{USR}_{IST}(u,t)-\hat{\eta}_{el,t}\cdot P^{IST}_{USR}(u,t)-P^{PV}(u,t)-P^{GRID}_{USR}(u,t)=0, \tag{4}$$

where

$$P_L^{USR}(u,t) = \hat{P}_{el}^{USR}(u,t) \cdot \alpha(u) + \frac{Q^{eh}(u,t)}{\hat{\eta}_{el,c}} \tag{5}$$

$$P^{PV}(u,t) = \hat{p}_{PV}(u,t) \cdot \sigma(u) \cdot \hat{A}_{PV}. \tag{6}$$

In Equation (5), Q^{eh} is the thermal power generated by the electric heater having efficiency $\hat{\eta}_{el,c}$. In Equation (6), $\hat{p}_{PV}$ is the electric production of each PV module per unit of the active surface area ($\hat{A}_{PV}$) and it is evaluated as shown in Appendix A.

IST thermal energy balance:

$$Q_L^{USR}(u,t) \cdot \alpha(u) - Q^{ST}(u,t) - Q^{eh}(u,t) - Q_{disch}^{TS}(u,t) + Q^{diss}(u,t) = 0, \tag{7}$$

where

$$Q_L^{USR}(u,t) = \hat{Q}_L^{sh}(u,t) + \hat{Q}_L^{dhw}(u,t) \tag{8}$$

$$Q^{ST}(u,t) = \hat{q}_{ST}(u,t) \cdot \chi(u) \cdot \hat{A}_{ST}. \tag{9}$$

In Equation (9), $\hat{q}_{PV}$ is the thermal production of each ST collector per unit of the active surface area ($\hat{A}_{ST}$) and it is calculated using Equation (A14) in Appendix A.

Note that the binary variable $\alpha(u)$ in Equations (5) and (7) is used to set the demand of a USR equal to zero when it is not selected to form the cooperative ($\alpha(u) = 0$).

Energy Flows Management

The following inequality constraints are included to obtain a proper and feasible management of the electric and thermal energy flows:

$$P_{ITS}^{USR}(u,t) \leq P^{PV}(u,t) \tag{10}$$

$$P_{ITS}^{USR}(u,t) \leq \left(\hat{P}_{el}(u,t) + \frac{\hat{Q}_L^{sh}(u,t) + \hat{Q}_L^{dhw}(u,t)}{\hat{\eta}_{el,c}} \right) \cdot \alpha(u) \tag{11}$$

$$Q^{eh}(u,t) \leq Q_L^{USR}(u,t) \cdot \alpha(u) \tag{12}$$

$$Q^{diss}(u,t) \leq Q^{ST}(u,t). \tag{13}$$

Equation (10) excludes the possibility of USRs sending to IST electricity purchased from the grid. Equations (11) to (13) exclude any interaction between IST and not-selected USRs. In particular, when a USR is not selected ($\alpha(u) = 0$), Equation (11) precludes IST from sending electricity to it ($P_{ITS}^{USR}(u,t) = 0$), its energy consumption for the electric heater is set to zero by Equation (12) ($Q^{eh}(u,t) = 0$), and its dissipated energy is null ($Q^{diss}(u,t) = 0$) if there is not renewable solar thermal energy production by Equation (13).

Roof Surface Management

The following constraints are included to guarantee a feasible occupation of the available roof surface:

$$\sigma(u) \cdot \hat{A}_{PV} + \chi(u) \cdot \hat{A}_{ST} \leq \hat{S}(u) \tag{14}$$

$$\sigma(u) \cdot \frac{\hat{A}_{PV}}{\hat{S}(u)} \leq \alpha(u) \tag{15}$$

$$\chi(u) \cdot \frac{\hat{A}_{ST}}{\hat{S}(u)} \leq \varepsilon(u) \tag{16}$$

$$\varepsilon(u) \leq \alpha(u) \tag{17}$$

where $\hat{S}(u)$ is the total available roof surface of the user u.

Equation (14) imposes that the combined PV and ST installations not cover more than the available roof surface. Equation (15) imposes that the number of PV modules of a not-selected USR is null. On the other hand, if a USR is selected, Equations (16) and (17) give priority to the PV modules rather than to the ST collectors.

IST as Storage

Since IST is modeled as a sink, it is capable of accepting all the energy generated by USRs that exceeds their consumption. Moreover, the campus is considered to behave like a daily storage system (Equations (18) and (19)); i.e., during the day, it would release up to the amount of energy it was charged with. When there is no production, IST can purchase energy from the grid and sell it to the respective USR, until all the stored energy during the day is returned (Equation (19)). To allow IST to send electricity to the USRs during the first part of the day (from midnight to sunrise, i.e., when there is no production from solar), each USR begins the day with an initial energy credit of 100 kWh.

Finally, Equations (20) and (21) mandate that the electricity cannot be flowing in both directions at the same time.

$$LVL^{IST}(u,t) = LVL^{IST}(u,t-1) + \hat{\eta}_{el,t} \cdot P^{USR}_{IST}(u,t) - P^{IST}_{USR}(u,t) \tag{18}$$

$$LVL^{IST}(u,0) \leq LVL^{IST}(u,23) \tag{19}$$

$$P^{IST}_{USR}(u,t) \leq \hat{M} \cdot s_{el}(u,t) \tag{20}$$

$$P^{USR}_{IST}(u,t) \leq \hat{M} \cdot (1 - s_{el}(u,t)) \tag{21}$$

In Equations (20) and (21), s_{el} is an auxiliary binary variable identifying the direction of electricity (when $s_{el}(u,t) = 1$ at time t, the electricity flows from IST to the USR u; when $s_{el}(u,t) = 0$, it flows in the opposite direction), and $\hat{M}$ is a very big constant parameter (no constraints on the maximum power that can be exchanged between IST and a USR is considered).

Thermal Storage Systems

The model of each thermal storage tank consists in two thermal energy balances, expressed in terms of the volume of hot water within the tank [11,12]: the first is between two subsequent hours (Equation (22)) and the second between the beginning and the end of the same day (the tank is considered a daily one, Equation (23)).

$$V^{TS}(u,t) = V^{TS}(u,t-1) + \frac{3600}{\hat{\rho}_w \hat{c}_{p,w}(T_h - T_c)} \cdot \left(\hat{\eta}_{TS} \cdot Q^{TS}_{disch}(u,t) - \frac{1}{\hat{\eta}_{TS}} Q^{TS}_{ch}(u,t) \right) \tag{22}$$

$$V^{TS}(u,0) = V^{TS}(u,23) \tag{23}$$

$$V^{TS}(u,0) \leq V^{TS}_{MAX}(u) \tag{24}$$

$$Q^{TS}_{disch}(u,t) \leq \hat{M} \cdot s_{th}(u,t) \tag{25}$$

$$Q^{TS}_{ch}(u,t) \leq \hat{M} \cdot (1 - s_{th}(u,t)). \tag{26}$$

The second term of Equation (22) is the sum of the volume of hot water stored in the previous hour and the variation of hot water volume during the current hour. This variation is found by transforming the difference between charged and discharged thermal flow rates into a difference between charged and discharged volumes (this operation requires the charged/discharged energy flow rates to be divided/multiplied by the round-trip efficiency $\hat{\eta}_{TS}$). Equation (23) is used to design the maximum capacity of the storages ($V^{TS}_{MAX}(u)$), which is an output of the optimization procedure. Inequalities in Equations (25) and (26) are akin to (20) and (21).

Economic Constraints

Finally, the constraint in Equation (27) imposes that—for the solution to be feasible—the USR has to save money compared to the case in which there is no intervention (i.e., it purchases all of the energy from the grid).

$$\sum_t \left(P_{USR}^{grid}(u,t) \cdot \hat{c}_{el}^{USR}(t) \right) \leq \sum_t \left(P_L^{USR}(u,t) \cdot \hat{c}_{el}^{USR}(t) \right) \quad (27)$$

2.4. Design/Operation Optimization Procedure

The design/operation procedure consists of the following three steps:

i. seasonal optimization,
ii. annual optimization, and
iii. calculation of the contribution of each USR category to the IST savings.

A sensitivity analysis is finally performed to evaluate the effects of the solar technology prices on the optimum results.

2.4.1. First Step: Seasonal Optimization

Four optimization runs (Section 2.3) are performed, one per each season of the year, to evaluate the optimum configuration of the system composed by the IST and the four selected USRs (each one representing a category of buildings) in each season. The results are the optimum value of the objective function (the IST costs, Equation (2)) and the optimum values of the decision variables, i.e.:

- the number of operating USRs;
- the number of PV modules of the selected USRs;
- the number of ST collectors of the selected USRs;
- the volume of the thermal storage; and
- the value of all the energy streams/quantities that are not fixed as parameters (i.e., electrical and thermal energy flows between nodes, thermal energy flows charged-to/discharged-from the thermal storages, and the level of charges of IST and thermal storages) in each time-step of the season.

2.4.2. Second Step: Annual Optimization

The operation of each of the four optimal design configurations found in the first step is optimized over the entire year, still in agreement with the minimization of the IST costs (Equation (2)). In each of these four operation optimizations, all the design variables are fixed at their "seasonal" optimum values found in the first step.

The resulting lowest optimum value of the objective function (IST yearly cost) is used to identify the best of the four design configurations.

2.4.3. Third Step: Calculation of the Contribution of Each USR Category to the IST Savings

The goal of the third step is twofold:

i. to calculate the share of the IST money savings each individual USR is responsible for, and
ii. to evaluate the potential money savings for IST considering all candidate buildings within a radius of 500m from the campus (that is considered an acceptable distance for the purpose of this study).

The money savings for IST (i.e., the reduction of its annual costs due to the installation of solar technologies, Equation (2) are the differences between the annual costs obtained from the optimization minus those in the reference case, in which there is no interaction between IST and USRs.

This goal is achieved by:

- performing a series of simulation runs with one USR at a time and calculating the money savings for IST. In this step, each USR includes the same number of PV panels and ST collectors of the design configuration identified in the second step,
- multiplying the obtained money savings associated with each USR by the total number of buildings belonging the USR category to get the total savings associated with this category of buildings, and
- summing the IST savings derived from the four categories of USRs/buildings to obtain the total money savings for IST in each season.

3. Results

The simulations were performed on a machine with an Intel® Core™ i7-2720QM CPU @ 2.20 GHz × 8 processor. The solving time of each simulation was about 0.5 s.

The reference case for the calculation of the money savings is the case of no-intervention: IST and the USRs are connected to the grid, and they purchase all the energy they need. In this case, the annual costs are IST 1,684,246 €, USR1 6581 €, USR2 4182 €, USR3 4991 €, and USR4 13,942 €.

3.1. First Step: Design Optimization in Each Season with All USRs

All seasonal optimizations (the first step of the design/operation optimization procedure described in Section 3) indicate the convenience of making all the four USRs interact with IST by installing only PV systems (i.e., it is never convenient to install ST collectors and TS capacity; the optimum value of $\chi(u)$ is always equal to 0).

The optimum number of PV modules ($\sigma^*(u)$ for u = USR1, ... ,USR4) is: (42,1,1, and 85) for winter; (42,59,35, and 85) for both spring and summer; and (29,8,1, and 54) for autumn.

In the spring-summer seasons, the rooftops of each category of buildings are to be completely covered by PV panels. Moreover, the highest optimum number of modules is always that of USR4 not only because of the largest available rooftop area (264 m^2, Table 1) but, also, thanks to the most favorable exposure (sud-oriented roof and less shadow cast by nearby buildings). This results in a high optimum number of modules even in winter (85, the same number as spring-summer) and autumn (54, 36% less than spring-summer). A similar result is obtained for USR1 (54 in winter and spring-summer vs. 29 in autumn), which also has a favorably exposed rooftop. On the contrary, the optimizations in winter and autumn show a very small optimum number of PV modules for USR2 and USR3 due to the less favorable exposure (their rooftops are east- and west-oriented, respectively).

3.2. Second Step: Annual Optimizations

In this section, the behaviors of the four optimum design configurations (all including PV modules only) obtained in the first step by the four seasonal optimization runs are simulated over the whole year (Table 2).

Table 2. Results of the second step: annual money savings for Instituto Superior Técnico (IST) and USRs, expressed as a percentage of the annual cost (1,684,246 €) in the reference case (no intervention).

Seasonal Optimum Design (Number of PV Modules)		IST	USR1	USR2	USR3	USR4
Winter	(42,1,1,85)	0.215	28.351	2.933	3.416	27.522
Spring-summer	(42,59,35,85)	0.274	28.351	24.472	28.780	27.522
Autumn	(29,8,1,54)	0.201	25.227	13.643	3.416	24.012

The design configuration that provides the maximum money savings for IST (best configuration) is the spring-summer one, which has the rooftops of the four selected USRs completely covered by PV modules. This configuration also provides the highest money savings for all USRs (in the range

24% to 28%). The savings for IST (0.274%) are obviously smaller, because the only power generated by the single four USRs is considered in this second step, which is much smaller than the IST energy requirements. The discussion on the extension of the number of users is made in Section 3.3.

Table 2 shows also that the IST annual money savings for the winter and autumn design configurations are significantly lower than those of the spring-summer configuration, mainly because of the strong drop of USR2 and USR3 savings (due to the lower optimum number of PV modules).

The total installed capacity in the chosen design configuration (summer-spring) is 64.09 kWp and results in an initial investment of 128,180 €.

The electricity purchased by IST from the grid during the PV production time is lower than that of the reference case, while it increases at the peak electricity demand of the USRs, as shown in Figure 6. It can be seen that, in autumn and winter, when the sunset occurs before the *ponta* phase (18:00 to 20:30), the variation of electricity purchased is null; IST "waits" for the most expensive phase to finish before feeding back the USRs with the energy it has accumulated. During this period, the USRs purchase all the electricity they need from the grid.

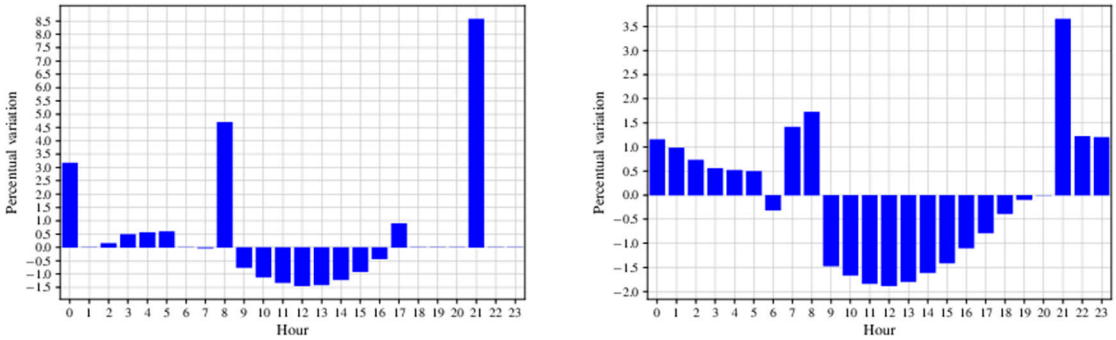

(**a**) (**b**)

Figure 6. IST percentage variation of the energy purchased from the grid compared with the reference case for the winter (**a**) and summer (**b**) seasons.

Results show also that, from the energy point of view, USR2 is the most suitable user for integration with IST; its electricity demand profile is not very different from that of USR3 (see Figure 5), but the amount of the stored energy profile is remarkably different, as in Figure 7. This is due to the different and opposite azimuth angles of the surfaces; the USR2 peak of PV generation can cover the morning peak of demand (completely in the spring and summer and partially in autumn) thanks to the east orientation of its rooftop; on the other hand, the USR3 surface orientation (west) does not provide benefits with respect to the evening peak (at 20:00).

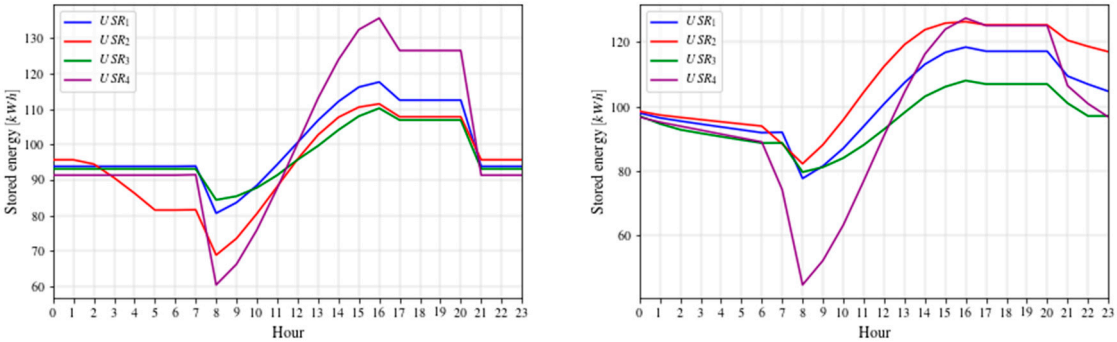

(**a**) (**b**)

Figure 7. Level of charge for IST as a storage system for the winter (**a**) and autumn (**b**) seasons.

IST is considered as a fictitious storage system; the campus can receive unlimited amounts of energy and release as much as it is convenient. In this framework, on the IST perspective, the most attractive partners would be those that make the level of charge increase from the beginning to the end of the day. USR2 is the most attractive in the set of USRs in this regard; it is the only one giving a positive contribution to the daily energy stored by IST for every season, except winter (Figure 7b). These results suggest that, for such electricity consumption profiles and tariffs, USRs with east-oriented surfaces are preferable for IST.

3.3. Third Step: Contribution of Each Category of USRs to the IST Savings

In the third step of the design/operation procedure, the simulations are run with a system comprising IST and only one USR at a time, each with the same number of equipment installed as in the best configuration resulting from the second-step solution. In this condition, the IST money savings, due to the association to each USR, are: 0.0662% for USR1, 0.0317% for USR2, 0.0368% for USR3, and 0.1383% for USR4. The sum of all of these terms is 0.273%, i.e., approximately equal to the total savings calculated with all USRs interconnected with IST (0.274%, Table 2). Therefore, it looks acceptable to consider the contribution of each category of USRs as independent of the others and, therefore, to calculate the IST total savings as the sum of the individual contributions of each USR.

It has been estimated that, in a radius of 500m from the campus, there is an amount of 31 buildings that fit for the category USR1, 16 for USR2, 12 for USR3, and 41 for USR4. The overall potential of IST money savings for each USR category is therefore: 2.052% for USR1, 0.507% for USR2, 0.442% for USR3, and 5.670% for USR4, for a total of 8.671% (146.046 k€), with 6151 modules installed, for an initial investment of 3.568 M€.

More buildings may be included, so that the overall savings be higher, but this might lead to a situation in which IST receives more energy than it requires (at peak production hours), making invalid the IST-as-sink hypothesis.

3.4. Sensitivity Analysis

A sensitivity analysis has been performed by varying the specific costs per PV module (c_{PV}) between 3 €/Wp and 1 €/Wp. Results are presented in Table 3. The same has been done for the ST and TS systems, but those equipment are not part of the optimal solution, even with a cost of 200 € per collector and 500 €/m^3, respectively.

Table 3. Results of the sensitivity analysis: percentage savings obtained with the optimal solutions for different values of the specific costs of the photo-voltaic (PV) modules (c_{PV}).

c_{PV} (€/Wp)	IST	USR1	USR2	USR3	USR4
3.0	0.042	17.118	5.989	14.194	16.774
2.5	0.123	24.755	16.491	19.320	24.012
2.0	0.276	28.351	24.472	28.780	27.522
1.5	0.493	28.351	24.472	28.780	27.522
1.2	0.625	28.351	24.472	28.780	27.522
1.1	0.669	28.351	24.472	28.780	27.522
1.0	0.713	28.351	24.472	28.780	27.522

The specific costs for the PV technology have been taken from [36]. In addition to that, two more cases have been examined: those in which the specific costs are 2.5 and 3 €/Wp, for which the optimal configuration of PV modules for USR1 to USR4 is 15,3,9, and 31 and 27,10,13, and 54, respectively.

Results show that the cost per watt peak affects the yearly savings of the campus, whereas those of the USRs remain unaffected when the number of modules installed do not change, because this cost is entirely financed by IST. Thus, the USR savings are affected only when the cost per unit module is high enough that it is not convenient to exploit completely the available surface. The savings for

IST are inversely proportional to the unitary cost of the PV modules, whereas, for the USRs, they are proportional to the available surfaces they can offer.

For the lowest specific price of the PV technology, the third step of the design/operation procedure shows that the overall saving potential for IST is 20.878%, with an initial investment of 1.784 M€.

4. Discussion

The system under analysis has been modeled under some assumptions. Each one is reasonable and is made to simplify the procedure, while, at the same time, keeping a good level of accuracy. However, the following considerations may help understand the limit of these assumptions and suggest directions for development also in applications different from the presented one.

The design day technique is very useful, because it reduces the complexity of the simulations (solving time), but it comes with the drawback of neglecting the positive and negative peaks in energy consumption and environmental conditions. Moreover, the design days are simulated independently; further studies should focus on the consequential simulation of time periods of at least a week long to appreciate the variations from day-to-day and from weekdays-to-weekends. Thermal loads are obtained from an approximation of the geometry of the residential complexes. This procedure can be performed with publicly available data and does not require accessing technical maps, but its accuracy on the amount of electrical and thermal energy used might be insufficient for the actual design of the systems.

The advantages of the ST systems depend on both the correct characterization of the thermal loads and the accuracy of the model describing their behavior. Different results may be obtained with different modeling techniques—i.e., nonlinear programming—and iterative solution processes.

Further assessments should include the possibility to install micro and/or mini-CHP or CCHP systems in IST for the self-production of electric, heating, and cooling energy; these systems would work for many hours per year at rated loads, since IST base electricity consumption is about 800 kW, and also, the energy spent for HVAC during the day might justify cogenerative solutions.

IST makes a profit by purchasing energy from the grid at night and selling it to the USRs at the same price they would normally buy it; this condition might not be acceptable for the grid management company, thus possibly changing the feasibility of the project.

The last remark is that it has been assumed that the behavior of the residents does not change after the intervention; with the possibility of self-consuming the free renewable energy during the day, the electrical energy usage might increase. To avoid a decrease in residential energy efficiency because of the increase in renewable energy generation, compensating mechanisms and conditions should be investigated. For example, IST may demand a maximum (fixed or variable) share of renewable energy for the USR self-consumption or a variable cost of the "discharged" energy, according to the quantity it has received.

5. Conclusions

This work presents an economic assessment of the design of a distributed PV system supplying with renewable electric energy the residential complexes on which the equipment is installed and the university campus that finances the project. Four typical buildings have been studied as representatives of a wide number of residential complexes present locally. The campus was described by an electric consumption profile based on measured data. The geometry and occupancy of the residential complexes were estimated from publicly available data, such as the number of floors, apartments per floor, and roof surfaces. According to these estimates, an electric consumption profile obtained from the measurements was associated with each apartment. Similarly, the thermal load for space heating was estimated on the basis of the general thermal characteristics of the buildings and environmental recorded data, whereas that for the domestic hot water was calculated as a function of the number of inhabitants. Two candidate technologies for energy generation were considered: photo-voltaic modules and solar thermal collectors with thermal storage. Both have been modeled with a basis on the

environmental data (hourly solar radiation and external temperature) and technological parameters. From all the data, four design days have been generated, each representative of a season of the year.

A MILP model was built to find the optimal design configuration of the system made up of IST and the four selected users/producers, the objective function being the yearly energy-related costs of IST.

Results show that photo-voltaic is the only convenient technology, whereas the solar thermal equipment are never part of the optimal solutions. It has been evaluated that, in a radius of 500 m from the campus, there is an estimated total amount of 100 buildings having the characteristics of the four selected users. If the total roof surface of these buildings is covered by PV modules, for a total of 6151 modules at 580 € each, IST, with an initial investment of 3.568 M€, benefits from a reduction of the yearly energy expenses of 8.671%, which equals to a savings of about 146.046 k€ per year during the module's expected lifetime (15 years). The highest share of money savings is for the USRs, each of which saves between 24.47% and 28.78%.

With this intervention, the energy consumption of both the campus and the residents is reduced when the energy costs are at their highest. The campus also returns partially or completely the energy received when there is no renewable generation and the cost of energy is lower. The East-side surface orientation has shown to be preferable, for it anticipates the renewable energy production covering the domestic peak load and allows the campus to receive more energy than the amount returned during the off-peak phase.

A sensitivity analysis on the unitary prices of the technologies was performed. The solar thermal technology is again never part of the optimal solution also when their prices are lowered reasonably. The residential savings depend on the number of installed modules, whereas the campus ones depend on the specific costs of the technology. To higher specific prices of the PV modules correspond a decrease in the number of installed equipment, hence a reduction in economic benefits for both IST and the USRs; the least favorable examined scenario was with a unitary price of 3 €/Wp, and under these conditions, the total number of installed modules was 1892. The yearly profit for IST is 1.263%, about 21.3 k€/year. The USRs savings decrease too, but the minimum one is still 17.5%. On the other hand, in the most favorable scenario, where the cost is 1 €/Wp, the investment cost is only 1.784 M€, and the yearly profit for IST is 20.878%, corresponding to 351.636 k€, the USR savings being the same as the base case.

The MILP model is simple and allows the assessment of many buildings one-by-one. The accuracy of the results can be enhanced with an improved characterization of the residential complexes and their energy flows and an analysis based on extended real-time periods. Smart procedures, conditions, and constraints should be investigated in all future works to avoid the development of energy-inefficient practices as a result of the availability of free renewable energy.

Author Contributions: Conceptualization, all authors; methodology, S.R. and S.C.; software, S.C.; formal analysis, A.L. and S.R.; investigation, S.C. and C.S.S.; data curation, S.C., C.S.S., and S.R.; writing—original draft preparation, S.C., A.L., and S.R.; writing—review and editing, A.L., S.R., and C.S.S.; visualization, S.C.; and supervision, A.L. and C.S.S. All authors have read and agreed to the published version of the manuscript.

Funding: This research received no external funding.

Conflicts of Interest: The authors declare no conflicts of interest.

Nomenclature

Roman symbols

A	area, m^2
C	cost, €
c	specific cost, €/Wp
g	equality constraints
h	inequality constraints
L	specific heat loss coefficient, kW/m^2

LVL	level
N	number
P	electric energy, kWh
Q	thermal energy, kWh
Rev	revenues, €
S	available surface area, m^2
s	season
T	temperature, °C
t	time, h
u	set identifying each user
V	volume, m^3
x	array of the decision variables' optimum value
Z	objective function

Greek symbols

α	binary variable, existence or not of a USR
ε	binary variable, inclusion or not of a ST technology
σ	integer variable, number of photo-voltaic modules
χ	integer variable, number of solar thermal collectors

Subscripts and superscripts

ch	charged
disch	discharged
diss	dissipated
eh	electric heating
el	electric
grid	electric grid
inv	investment
IST	Instituto Superior Técnico (campus)
L	load
O&M	operation and maintenance
PV	photo-voltaic
sh	space heating
ST	solar thermal
TS	thermal storage
USR	user

Appendix A. Model of the Solar Energy Production

This Appendix presents the process performed to obtain the electrical and thermal output energy for a PV module and ST collector, respectively. The calculations, as well as the nomenclature, are the same as [31,33].

The inputs are hourly median hourly values for solar radiation and temperature, obtained with the same process presented in Section 2.1.2. It is assumed that the modules will be oriented according to the normal of the façade of the building they will be installed on; therefore, each USR will have a different specific solar energy production profile. All of the angles in the calculations are in radians.

Appendix A.1. Incident Solar Radiation on a Surface

All the calculations revolve around the solar time, and the daylight savings time (DST) has not been taken into account.

The incident angle (θ) the sun has with a tilted surface is calculated as:

$$\begin{aligned}\cos\theta = \quad & \sin\delta\sin\varphi\cos\beta - \sin\delta\cos\varphi\sin\beta\cos\gamma + \cos\delta\cos\varphi\cos\beta\cos\omega_m \\ & + \cos\delta\sin\varphi\cos\gamma\cos\omega_m + \cos\delta\sin\beta\sin\gamma\sin\omega_m\end{aligned} \tag{A1}$$

being δ the solar declination, φ Lisbon's latitude, β and γ the slope and the azimuth angles of the rooftop surface, and ω_m the midpoint between two subsequent hour angles (ω_1 and ω_2).

If sunrise (sunset) occurs in between two subsequent hour angles, then ω1 (ω2) assumes the value of the sunrise (sunset) hour angle, while ω2 (ω1) is unchanged.

The measured irradiance (I) and the extraterrestrial irradiance on a horizontal surface, between sunrise and sunset (I_0), can be calculated from the measured values of the solar radiation (G) and the calculated values of the extraterrestrial radiation incident on the plane normal to the radiation (G_{on}).

$$I = G \cdot \left(\frac{\deg(\omega_2 - \omega_1)}{15 \cdot 3600} \right) \tag{A2}$$

$$I_0 = \frac{24 \cdot 3600}{2\pi} G_{on} (\cos\varphi \cos\delta (\sin\omega_2 - \sin\omega_1) + (\omega_2 - \omega_1) \sin\varphi \sin\delta) \tag{A3}$$

The isotropic sky model has been chosen for modeling the incident radiation on a sloped surface due to its simplicity and effectiveness [31]. The model relies on the assumption that the radiation is made of three components: beam, isotropic diffuse, and diffused ground-reflected radiation. The total solar radiation on a tilted surface for an hour is the sum of the tree terms:

$$I_T = I_b R_b + I_d \left(\frac{1 + \cos\beta}{2} \right) + I\rho_g \left(\frac{1 - \cos\beta}{2} \right) \tag{A4}$$

R_b is the ratio of beam radiation on the plane to that on an horizontal surface:

$$R_b = \frac{\cos\theta}{\cos\theta_z} \tag{A5}$$

$$\cos\theta_z = \cos\delta \cos\omega_m \cos\varphi + \sin\delta \sin\varphi \tag{A6}$$

In some days, the sunset/sunrise occurs closely enough to the beginning of the following, thus resulting in very low values of $\cos\theta_z$. The ratio has therefore been limited to a maximum value of 30 in order not to have impossible values of the beam radiation.

I_d is the isotropic diffuse radiation, which is found by the following correlation:

$$\frac{I_d}{I} = \begin{cases} 1.0 - 0.09 k_T & \text{for } k_T \leq 0.22 \\ 0.9511 - 0.1604 k_T + 4.388 k_T^2 - 16.638 k_T^3 + 12.336 k_T^4 & \text{for } 0.22 < k_T \leq 0.8 \\ 0.165 & \text{for } k_T > 0.22 \end{cases} \tag{A7}$$

k_T being the clearness index, defined as:

$$k_T = \frac{I}{I_0} \tag{A8}$$

Again, for short timespans, values of k_T higher than 1 can be obtained. This is impossible, because it would mean that the total radiation arriving on the Earth's surface (I) is greater than the total extraterrestrial radiation (I_0), which is impossible and is a consequence of working with small time intervals; therefore, all the values have been rounded down to 1 when necessary.

Eventually, the total radiation incident on a tilted surface is obtained with:

$$G_T = I_T \cdot \left(\frac{15 \cdot 3600}{\deg(\omega_2 - \omega_1)} \right) \tag{A9}$$

Appendix A.2. PV Electricity Production

The selected PV technology is a monocrystalline silicium (mono-SI) panel manufactured by [32]. The power output of a PV module is modeled as a function of the incident solar radiation and the ambient temperature as proposed by Durisch et al. [33].

The efficiency is:

$$\eta_{PV} = p \cdot \left[q \frac{G_T}{G_{T,ref}} + \left(\frac{G_T}{G_{T,ref}} \right)^m \right] \cdot \left[1 + r \frac{T_M}{T_{M,ref}} + s \frac{am}{am_{ref}} + \left(\frac{G_T}{G_{T,ref}} \right)^u \right] \tag{A10}$$

where $G_{T,ref} = 1000\ W/m^2$ is the reference solar radiation, $T_{M,ref} = 25\ C$ is the reference module temperature, and $am_{ref} = 1.5$ the reference air mass. The coefficients p, q, r, s, and u for mono-Si modules are equal to 0.2362, 0.2983, 0.9795, and 0.9865 [33], respectively.

The air mass is calculated as:

$$am = \frac{\exp(-0.0001184h)}{\cos\theta_z + 0.5057} \tag{A11}$$

While the module temperature as:

$$T_M = T_{amb} + h \cdot G_T \tag{A12}$$

being h equal to 0.028 for the mono-SI modules [33]. All the temperatures are expressed in °C. The specific direct current (DC) power output of a PV module is eventually calculated as:

$$p_{PV} = G_T \cdot \eta_{pv} \cdot \eta_{inv} \frac{1\ W}{1000\ kW} \tag{A13}$$

where η_{inv} is the inverter efficiency equal to 98%.

Appendix A.3. ST Thermal Power Production

The solar thermal energy output does not only depend on the physical properties of the collector itself but, also, on the inlet fluid temperature. This changes accordingly with the temperature inside the TS (which depends on the tank capacity and the energy subtraction from the users).

The heat generated by a collector per unit of collector area, q_{ST}, is:

$$q_{ST} = \dot{m}_f c_p \left(T_{f,o} - T_{f,i}\right) = F_R(\tau \cdot \alpha) G_T - F_R U_L \left(T_{f,i} - T_{f,amb}\right) \tag{A14}$$

where $\dot{m}_f$ is the mass flow rate of the heat transfer fluid (water-glycol), c_p its specific heat, $T_{f,o}$ and $T_{f,i}$ its outlet and inlet temperatures, F_R is the heat removal factor, and U_L is the overall heat loss coefficient. Here, $F_R(\tau \cdot \alpha) = 0.68$ and $F_R U_L = 4.9$ [37].

References

1. International Energy Agency. Renewables Information 2018. OECD. 2018. Available online: https://doi.org/10.1787/renew-2018-en (accessed on 1 October 2018).
2. European Commission Photovoltaic Geographical Information System, Global Irradiation and Solar Electricity Potential. Available online: http://re.jrc.ec.europa.eu/pvg_download/map_index (accessed on 1 October 2018).
3. Mohammadi, M.; Noorollahi, Y.; Mohammadi-ivatloo, B.; Yousefi, H. Energy hub: From a model to a concept—A review. *Renew. Sustain. Energy Rev.* **2017**, *80*, 1512–1527. [CrossRef]
4. Alarcon-Rodriguez, A.; Ault, G.; Galloway, S. Multi-objective planning of distributed energy resources: A review of the state-of-the-art. *Renew. Sustain. Energy Rev.* **2010**, *14*, 1353–1366. [CrossRef]
5. Chicco, G.; Mancarella, P. Distributed multi-generation: A comprehensive view. *Renew. Sustain. Energy Rev.* **2009**, *13*, 535–551. [CrossRef]
6. Sameti, M.; Haghighat, F. Optimization approaches in district heating and cooling thermal network. *Energy Build.* **2017**, *140*, 121–130. [CrossRef]
7. Orehounig, K.; Evins, R.; Dorer, V. Integration of decentralized energy systems in neighbourhoods using the energy hub approach. *Appl. Energy* **2015**, *154*, 277–289. [CrossRef]
8. Sigarchian, S.G.; Malmquist, A.; Martin, V. The choice of operating strategy for a complex polygeneration system: A case study for a residential building in Italy. *Energy Convers. Manag.* **2015**, *163*, 278–291. [CrossRef]
9. Fetanat, A.; Khorasaninejad, E. Size optimization for hybrid photovoltaic–wind energy system using ant colony optimization for continuous domains based integer programming. *Appl. Soft Comput.* **2015**, *31*, 196–209. [CrossRef]
10. Christidis, A.; Koch, C.; Pottel, L.; Tsatsaronis, G. The contribution of heat storage to the profitable operation of combined heat and power plants in liberalized electricity markets. *Energy* **2012**, *41*, 75–82. [CrossRef]
11. Rech, S.; Lazzaretto, S. Smart rules and thermal, electric and hydro storages for the optimum operation of a renewable energy system. *Energy* **2018**, *147*, 742–756. [CrossRef]
12. Rech, S. Smart Energy Systems: Guidelines for Modelling and Optimizing a Fleet of Units of Different Configurations. *Energies* **2019**, *12*, 1320. [CrossRef]
13. Wolsey, L.A. *Integer Programming*, 1st ed.; John Wiley & Sons: Hoboken, NJ, USA, 1998.
14. Omu, A.; Hsieh, S.; Orehounig, K. Mixed integer linear programming for the design of solar thermal energy systems with short-term storage. *Appl. Energy* **2016**, *180*, 313–326. [CrossRef]
15. Berkeley Lab. Distributed Energy Resources—Customer Adoption Model. Available online: https://building-microgrid.lbl.gov/projects/der-cam (accessed on 3 October 2018).

16. Jung, J.; Villaran, M. Optimal planning and design of hybrid renewable energy systems for microgrids. *Renew. Sustain. Energy Rev.* **2017**, *75*, 180–191. [CrossRef]
17. Braslavsky, J.R.; Wall, J.R.; Reedman, L.J. Optimal distributed energy resources and the cost of reduced greenhouse gas emissions in a large retail shopping centre. *Appl. Energy* **2015**, *155*, 120–130. [CrossRef]
18. Stadler, M.; Groissböck, M.; Cardoso, G.; Marnay, C. Optimizing distributed energy resources and building retrofits with the strategic DER-CAModel. *Appl. Energy* **2014**, *132*, 557–567. [CrossRef]
19. GAMS Software GmbH. An Introduction to Gams. Available online: https://www.gams.com/products/introduction/ (accessed on 3 October 2018).
20. IBM. IBM ILOG CPLEX Optimization Studio CPLEX User's Manual. Available online: https://www.ibm.com/support/knowledgecenter (accessed on 3 October 2018).
21. Gurobi Optimization, LLC. Gurobi Optimizer Reference Manual. Available online: http://www.gurobi.com/documentation/8.0/refman/index.html (accessed on 3 October 2018).
22. Instituto Superior Técnico. Campus Sustentável. Available online: http://sustentavel.unidades.tecnico.ulisboa.pt (accessed on 4 October 2018).
23. Rech, S.; Toffolo, A.; Lazzaretto, A. TSO-STO: A two-step approach to the optimal operation of heat storage systems with variable temperature tanks. *Energy* **2012**, *45*, 366–374. [CrossRef]
24. Stavropoulos, A.S. Spatial Analysis of Heating and Cooling Energy Needs in Lisbon. Master's Thesis, Instituto Superior Técnico, Lisbon, Portugal, 2013.
25. Municípia and Lisboa E-Nova. Carta de Potencial Solar. Available online: http://80.251.174.200/lisboae-nova/potencialsolar/ (accessed on 5 October 2018).
26. ADENE. Medidas Ppec 2013–2014. Available online: https://www.adene.pt/comportamentos/medidas-ppec-2013-2014/ (accessed on 5 October 2018).
27. Assembleia da República. *Regulamento das Características de Comportamento Térmico dos Edifícios (RCCTE)*; Diário da República—I Série A n° 67; Assembleia da República: Lisbon, Portugal, 2006; pp. 2468–2513. (In Portuguese)
28. Durmayaz, A.; Kadıoğlu, M.; Şen, Z. An application of the degree-hours method to estimate the residential heating energy requirement and fuel consumption in Istanbul. *Energy* **2000**, *25*, 1245–1256. [CrossRef]
29. Assembleia da República. *Regulamento de Desempenho Energético dos Edifícios de Habitação (REH)*; Diário da República-Série I-A; Assembleia da República: Lisbon, Portugal, 2013; pp. 2468–2513. (In Portuguese)
30. Santos, A.D.S. Avaliação de Sistemas Solares Térmicos de Produção de Água Quente Sanitária em Edifícios de Habitação Multifamiliar. Master's Thesis, Instituto Superior Técnico, Lisbon, Portugal, 2012. (In Portuguese)
31. Duffie, J.A.; Beckman, W.A. *Solar Engineering of Thermal Processes*; John Wiley & Sons: Hoboken, NJ, USA, 2013.
32. Sunmodule Plus SW 290 Mono (5-Busbar) Photovoltaic Module. Available online: https://web.archive.org/web/20181014162534 (accessed on 1 October 2018).
33. Durisch, W.; Bitnar, B.; Mayor, J.C.; Kiess, H.; Hang Lam, K.; Close, J. Efficiency model for photovoltaic modules and demonstration of its application to energy yield estimation. *Sol. Energy Mater. Sol. Cells* **2007**, *91*, 79–84. [CrossRef]
34. Lamedica, R.; Santini, E.; Ruvio, A.; Palagi, L.; Rossetta, I. A MILP methodology to optimize sizing of PV-Wind renewable energy systems. *Energy* **2018**, *165*, 385–398. [CrossRef]
35. Yokoyama, R.; Hasegawa, Y.; Ito, K. A MILP decomposition approach to large scale optimization in structural design of energy supply systems. *Energy Convers. Manag.* **2002**, *43*, 771–790. [CrossRef]
36. Villar, C.H.; Neves, D.; Silva, C.A. Solar PV self-consumption: An analysis of influencing indicators in the portuguese context. *Energy Strategy Rev.* **2017**, *18*, 224–234. [CrossRef]
37. Liu, B.Y.; Jordan, R.C. The long-term average performance of flat-plate solar-energy collectors. *Sol. Energy* **1963**, *7*, 53–74. [CrossRef]